THE ARCHIVE OF MECHANICAL ENGINEERING

Vol. LI 2004 Number 4

Key words: *propeller theory, propeller aerodynamics*

*PIOTR STRZELCZYK**)

METHOD OF CALCULATION OF NORMAL FORCE ON PROPELLER AT ANGLE OF ATTACK BY SIMPLIFED VORTEX METHOD

In the paper, the author presents a certain approach to the calculation of performance of the propeller exposed to inclined inflow conditions. The method presented in the paper employs the results of vortex of propeller for averaged velocity field as well as momentum and angular momentum theorem for the propeller wake. The blade element in the model is regarded as a source of tangential and axial force. Thanks to the approximation of lift force coefficient vs. angle of attack by sine curve one can get a quadratic equation for local, axial velocity component. The approach allows us to avoid an iterative solution for the induced velocities. The tangential induced velocity may be calculated from the relations obtained from vortex theory of propeller. A profile drag is incorporated to the calculation when the value of inflow angle is known. The presented method was compared with available data for propeller operating at angle of attack and in the axial inflow. The comparison showed good agreement with experimental data for the thrust and power coefficients for a wide range of advance ratios and blade settings, and angles of attack ranging from 0–15 degrees.

NOMENCLATURE

a_0	lift curve slope	1/rd
A	blade element shape parameter	–
B	number of bladesc	–
c	hord of the blade element	m
$C_{P_S} = P_S/(\rho n_S^2 D^4)$	thrust coefficient	–
$C_{P_N} = P_N/(\rho n_S^2 D^4)$	normal force coefficient	–

*) *Rzeszów University of Technology, ul. Wincentego Pola 2, 35-959 Rzeszow, Poland; E-mail: piostrz@prz.rzeszow.pl*

$C_N = N/(\rho n_s^3 D^5)$	power coefficient	–
$C_{M_z} = M_Z/(\rho n_s^2 D^5)$	yaw moment coefficient	–
C_X	drag coefficient	–
C_Z	lift coefficient	–
D	diameter of propellerm	m
F	Prandtl tip loss ratio	–
$J = V_\infty/n_s D$	advance ratio	–
$J' = J\cos\alpha_s$	reduced advance ratio	–
M	torque	Nm
Ma	Mach number	–
M_Z	yawing moment of propeller	Nm
n_s	propeller number of rotations per second	1/s
N	power	W
P_N	normal force	N
P_S	thrust force	N
r	radial coordinate	m
R	propeller tip radius	m
Re	Reynolds number	–
V_∞	freestream velocity	m/s
V_X	axial component of velocity at propeller disk	m/s
V_θ	tangential component of induced velocity at propeller disk	m/s
W	inflow velocity at the blade element	m/s

Greek letters:

α	blade-section angle of attack	rd
α_0	blade-section zero-lift angle of attack	rd
α_s	propeller angle of attack	rd
$\alpha^{(0)} = \alpha - \alpha_0$	blade-section aerodynamic angle of attack	rd
B	local blade setting angle	rd
$\beta^{(0)} = \beta - \alpha_0$	aerodynamic blade setting angle	rd
Γ	blade-section circulation	m^2/s
Γ_∞	circulation for infinite number of blades	m^2/s
H	efficiency of propeller	–
$\lambda = V_\infty/\omega R$	advance ratio coefficient	–
$\xi = r/R$	dimensionless radial coordinate	–
ξ_0	dimensionless hub radius	–
P	air density	kg/m^3

$\sigma = Bc/2\pi r \equiv B\bar{c}/2\pi\xi$	local solidity of propeller	–
Φ	local inflow angle	rd
$\chi_p = C_Z/a_0 \sin\alpha^{(0)}$	blade-element "efficiency"	–
ψ	blade azimuth angle	rd
ω	angular velocity of propeller axis	rd/s

1. Introduction

The problem of determination of the normal force on propeller is of interest of both aeronautical [2], [10], [15] and marine engineers [6]. In real flight, propeller works at some angle of attack α_S (see: Fig. 1) forced by geometrical angle of attack of the wing of airplane, and induced velocity generated by wing (or other parts of aircraft). For the tractor propeller, the effective angle of attack will be increased by the wing induced velocities, whereas for the pusher propeller the effective angle of attack will be diminished. In the case of small fast ships, some design reasons lead to the propeller inclination of the propeller shaft. The inclination is even increased by the trim of the boat, when she moves at high speed. The goal of the presented work was to develop a simple method of calculation of the performance of the propeller working at the angle of incidence.

The most common method [2], [10], [15] of estimating the normal force on propeller has been given by Ribner [13]. The method took into account the effect of propeller induced velocities and parasite drag of the blade. Another method has been proposed by McCormick [10]. However, the author of the method assumes constant chord of blade and averaged constant drag coefficient along the blade span. Hall [5] has given a method of analysis of propeller performance at angle of attack based on combined blade element and momentum theory originally developed by McCormick [9] for propeller in axial inflow. He also introduced tip loss coefficient for skewed propeller wake. In the original paper by Hall, one may find that for small angles of attack (± 15) the values of tip loss coefficients are nearly the same as Prandtl tip-loss factor [3] The induced velocities must be calculated making use of iterative method, similary to the Glauert method [3]. Szantyr [6] developed a method of design and analysis of marine propeller working in the inclined flow. His approach was based on lifting line method employing Goldstein tip loss factors [4], [6]. The lift curve as well as polar curve of hydrofoil were corrected for cavitation.

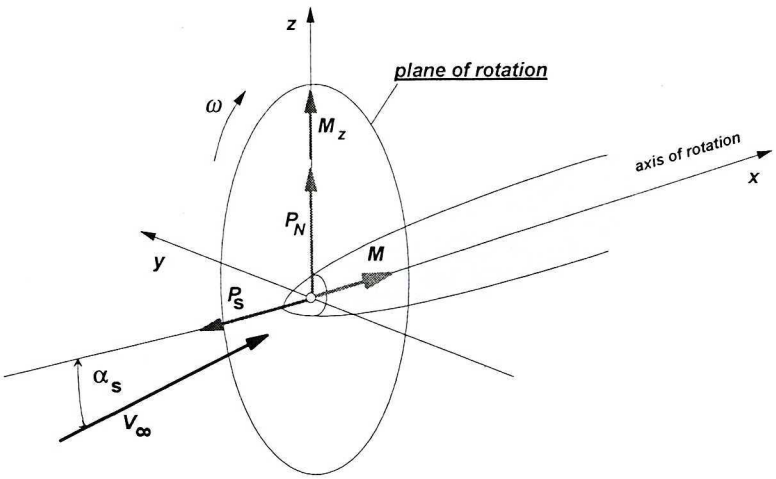

Fig. 1. Propeller at angle of attack

Recently, Phillips et al. [13] have developed a method of analysis of propeller performance in inclined flow. Their model is also based on lifting line model making use of Prandtl tip loss factor. The model assumes small incidence of propeller, as well as linear lift curve. The iterative solution procedure for induced inflow angle is nearly the same as described in [6], [12].

The method of calculation of propeller performance in inclined flow proposed by the author may be regarded as a generalization of earlier method developed for the propeller analysis in axial inflow [17]. The model couples a local momentum and angular momentum theorem with lifting line model with Prandtl (or Goldstein) tip loss factor. Thanks to sinusoid representation of the lift curve [14], [17], an analytical solution both for axial and tangential induced velocities for given radius and azimuth of the blade is possible. After calculation of angle of inflow, one may find lift and drag of airfoil. Hence, after numerical integration of the blade element forces one may obtain general propeller characteristics. There is no additional assumptions on values of induced velocities, like in [13].

2. Basic equations of the model

The model of the propeller flow applied for the present method is based on the following assumptions:

- Profile drag is neglected in the flow analysis;
- The lift curve is described by sinusoid as in eqn. (14);
- The blade element is a source of local axial and tangential forces;
- The velocity induced by bound vortices can be neglected;

- The tangential and axial components of induced velocity in the far wake are two times larger than at the actuator disk;
- The pressure at the far wake is equal to the ambient pressure.

The scheme of the inflow conditions on the propeller disk is presented in Fig. 1.

The circulation of the velocity around single blade of the B-blade propeller is coupled with circulation of the averaged velocity field by Prandtl tip loss factor F:

$$F = \frac{B\Gamma}{\Gamma_\infty} \tag{1}$$

The value of tip loss factor [3] is given by formula:

$$F = \frac{2}{\pi}\arccos\left(\exp\left(\frac{B}{2}\frac{\xi - 1}{2\sin\phi_T}\right)\right) \tag{2}$$

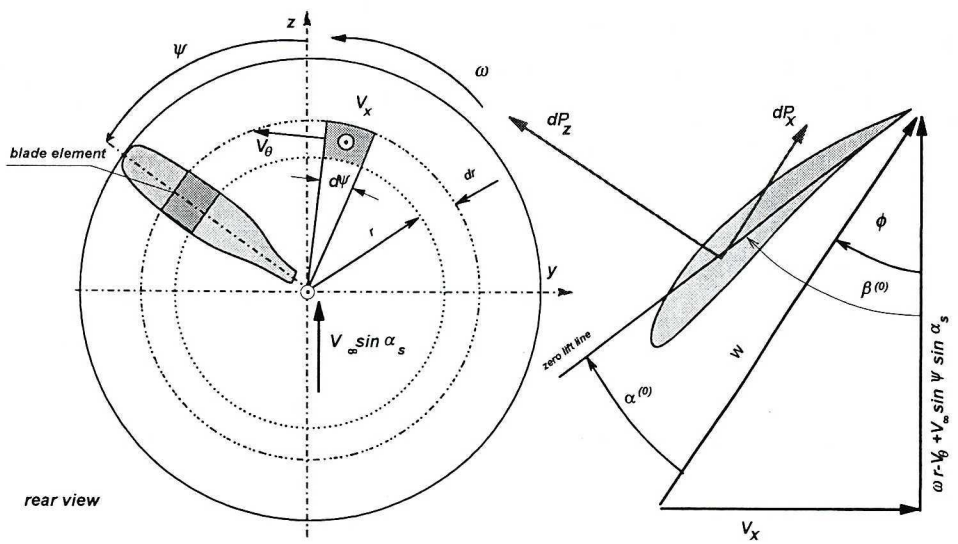

Fig. 2. Flow through the actuator disk and forces at the blade element. Schematic

Making use of Joukowski theorem, the elementary thrust and torque for the blade element of ideal propeller may be written in the following form:

$$\frac{d^2 P_{Sid}}{dr d\psi} = \frac{B}{2\pi}\rho W\Gamma\cos\phi \tag{3}$$

$$\frac{d^2 M_{id}}{dr d\psi} = \frac{B}{2\pi}\rho W\Gamma r\sin\phi \tag{4}$$

Employing momentum theorem to the elementary streamtube associated to the analyzed blade element one may get the following two equations:

$$\frac{d^2 P_{Sid}}{dr d\psi} = 2\rho V_X (V_X - V_\infty \cos\alpha_s) rF \tag{5}$$

$$\frac{d^2 M_{id}}{dr d\psi} = 2\rho V_X V_\theta r^2 F \tag{6}$$

The geometric relationships shown in Fig. 2. allow us to rewrite equations (3) and (4) in the following form:

$$\frac{d^2 P_{Sid}}{dr d\psi} = \rho \frac{B}{2\pi} \Gamma (\omega r + V_\infty \sin\alpha_s \sin\psi - V_\theta) \tag{7}$$

$$\frac{d^2 M_{id}}{dr d\psi} = \rho \frac{B}{2\pi} \Gamma V_X r \tag{8}$$

Inserting right hand sides of (5) and (6) to (7) and (8) respectively, one may get the following relations:

$$B\Gamma = 4\pi r V_\theta F \tag{9}$$

and:

$$V_x (V_x - V_\infty \cos\alpha_s) = (\omega r + V_\infty \sin\alpha_s \sin\psi - V_\theta) V_\theta \tag{10}$$

Because the swirl component of induced velocity is usually small in comparison with ωr and axial velocity V_X, equation (10) may be linearised, neglecting term V^2_θ as a small of the second order [1]. Hence, the relationship between axial inflow V_X and tangential induced velocity takes form:

$$V_\theta = \frac{V_x (V_x - V_\infty \cos\alpha_s)}{\omega r + V_\infty \sin\alpha_s \sin\psi} \tag{11}$$

or in dimensionless form:

[1] Justification of this linearization may be found in [11],[18].

$$\bar{V}_0 = \frac{\bar{V}_X (\bar{V}_X - \lambda \cos \alpha_s)}{\xi + \lambda \sin \alpha_s \cos \psi} \tag{12}$$

Note that, for axial inflow, in the hypothetic case of constant axial component V_x, the far wake would rotate like two dimensional potential vortex ("hub vortex") with circulation: $\Gamma_h = 2\pi V_X (V_X - V_\infty)/\omega$. This agrees well with the results obtained from Biot-Savart law for averaged velocity field for vortex actuator disk model, after much more laborious calculations [1].
Circulation around the blade element may be expressed by the well known formula:

$$\Gamma = \frac{1}{2} W c C_Z \tag{13}$$

It is reasonable to express lift coefficient curve in the following form [14]:

$$C_Z = a_0 \chi_p (\alpha^{(0)}, Re, Ma) \sin \alpha^{(0)} \tag{14}$$

Equation (14) may be treated as a theoretical lift curve corrected for viscosity effects. Such a representation of lift curve is depicted in Fig. 3.

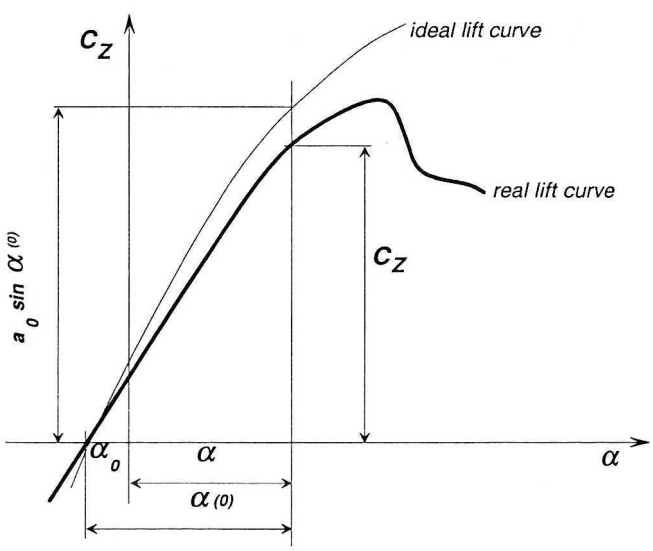

Fig. 3. The lift curve

Angle of attack measured from zero lift line is equal:

$$\alpha^{(0)} = \beta^{(0)} - \phi \tag{15}$$

From (13),(14),(15) and (9) one may get the following equation for dimensionless tangential component of induced velocity for given radial station and azimuth angle:

$$\bar{V}_\theta = A\left(tg\,\beta^{(0)} - \frac{\bar{V}_X}{\xi + \lambda \sin\alpha_s \sin\psi} \right) \tag{16}$$

Where "blade shape parameter" A is given by formula:

$$A = \frac{a_0 \chi_p \sigma \cos\beta^{(0)}}{4} \frac{(\xi + \lambda \sin\alpha_s \sin\psi)}{\left(F + \frac{a_0 \chi_p \sigma \sin\beta^{(0)}}{4} \right)} \tag{17}$$

Comparison of (12) and (16) leads to the quadratic equation for axial component of the velocity at the actuator disk. The solution of the equation is:

$$\bar{V}_X(\xi,\psi) = \frac{\lambda\cos\alpha_s - A}{2} + \sqrt{\left(\frac{\lambda\cos\alpha_s - A}{2} \right)^2 + A(\xi + \lambda \sin\alpha_s \sin\psi) tg\,\beta^{(0)}} \tag{18}$$

When the axial velocity is known, one may calculate tangential component of induced velocity from equation (12). Hence, the value of dimensionless inflow velocity $\bar{W}$ is given by the formula:

$$\bar{W} = \sqrt{\bar{V}_X^2 + (\xi + \lambda \sin\alpha_s \sin\psi - \bar{V}_\theta)^2} \tag{19}$$

The local inflow angle one may calculate from the following equation:

$$\phi(\xi,\psi) = arctg\,\frac{\bar{V}_X}{\xi + \lambda \sin\alpha_s \sin\psi - \bar{V}_\theta} \tag{20}$$

From equation (14) one may calculate angle of attack, and hence lift and drag coefficients C_Z and C_X.

The thrust, normal force and power coefficients may be calculated from the analysis of forces acting on bade element:

$$C_{P_S} = \frac{\pi^2}{8} \int_{\xi_0}^{1} \int_{0}^{2\pi} \bar{W}^2 \sigma \xi (C_Z \cos\phi - C_X \sin\phi)\, d\psi d\xi \tag{21}$$

Normal force coefficient:

$$C_{P_N} = \frac{\pi^2}{8} \int_{\xi_0}^{1} \int_{0}^{2\pi} \bar{W}^2 \sigma \xi (C_Z \sin\phi + C_X \cos\phi) \sin\psi\, d\psi d\xi \tag{22}$$

The work done by forces acting on propeller in the unit time is equal (Fig. 1.):

$$N = \vec{P} \bullet \vec{V}_\infty = P_S V_\infty \cos\alpha_s + P_N V_\infty \sin\alpha_s \tag{23}$$

The first part of the power is the useful power, whereas second term represents additional power which must be added to the total power of propeller. Hence, the power delivered by the power plant to the propeller is divided into the power dependent on torque and a part dependent on work of normal force. This last part of the power absorbed by propeller is analogous to the part of profile power of helicopter rotor in forward flight dependent on rotor advance ratio [7]:

$$N = \omega M + P_n V_\infty \sin\alpha_s \tag{24}$$

The power coefficient due to torque is equal:

$$C_{No} = \frac{\pi^3}{4} \int_{\xi_0}^{1} \int_{0}^{2\pi} \bar{W}^2 \sigma\, (C_Z \sin\phi + C_X \cos\phi)\, \xi^2 d\psi d\xi \tag{25}$$

and the power coefficient dependent on normal force:

$$C_{N_N} = C_{P_N} J \sin\alpha_s \tag{26}$$

Efficiency of propeller can be now calculated by formula:

$$\eta = \frac{C_{P_S}}{C_{No} + C_{N_N}} J \cos\alpha_s \tag{27}$$

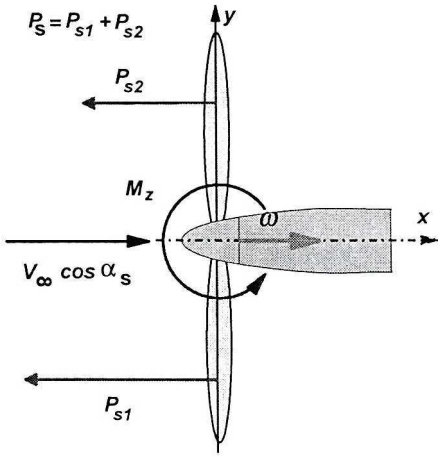

Fig. 4. Origin of yawing moment of propeller

Because thrust distribution is nonuniform (Fig. 4), the propeller produces yawing moment M_z.
The coefficient of the moment can be calculated from the formula:

$$C_{M_z} = \frac{\pi^2}{16} \int_{\xi_0}^{1} \int_{0}^{2\pi} \bar{W}^2 \sigma \xi^2 (C_Z \cos\phi - C_X \sin\phi)\, d\psi\, d\xi \tag{28}$$

3. Comparison of the present model with experimental data

To validate the model the experimental data presented in [11] have been employed. The report contains data from measurements of aerodynamic forces for four blade propeller with NACA 16-xxx blade sections The propeller was designed for relatively high advance ratio J = 4,0. Available are the following blade settings: 30°, 40°, 50°, 60° at r/R = 0,75. Some data are available also for 25° and 65° blade settings. The propeller angles of incidence were equal $\alpha_s = 0°$, 15°, 30°, 45°, 60°, 75°, 85° and 180° (like in helicopter vertical descent) Because of the constrains associated with skew of wake [5], the calculations were conducted only for the propeller incidences $\alpha_s = 0°$, 15°, 30° and blade settings: $\beta_{0,75} = 30°$, 40°, 50° for $\alpha_s = 0$.

This should cover the possible blade settings and angles of attack for a general aviation aircraft.
The power and thrust coefficients for symmetrical inflow conditions ($\alpha_s = 0°$) are shown in Figs. 5 and 6[1]. The agreement between calculations and

[2] In figures 5–12 symbols mean experimental data, and continuous lines mean the calculated values.

experimental data are very good for lower blade settings and below beginning of the blade stall (for advance ratios: 0,60; 1,4; 1,8 for $\beta_{0,75}=30°$; 40°; 50°, respectively). For the lower advance ratios, the method underestimates both thrust and power coefficients. The same problem occurs also for much more complicated models of propellers in axial flow [18]. For the propeller incidence $\alpha_s=15°$, one may observe the same behavior of thrust and power curves versus reduced advance ratio $J' = J\cos\alpha_s$ as in the case of purely axial inflow (Fig. 7 and 8). For the propeller incidence $\alpha_s=30°$, the agreement between calculations and experimental data is only good (Fig. 9 and 10).

The normal force coefficient shows very good agreement with experimental data for propeller incidence of 15 degrees, whereas for 30 degrees the agreement is poor (see Fig. 11 and 12). The same problem appears in the case of high blade setting $\beta_{0,75}=40°$.

The yawing moment of propeller shows behavior similar to the presented in [11], however, due to irregularities of curves $C_{Mz}(\beta_0, J')$ and its small values, the exact readings have been impossible to do.

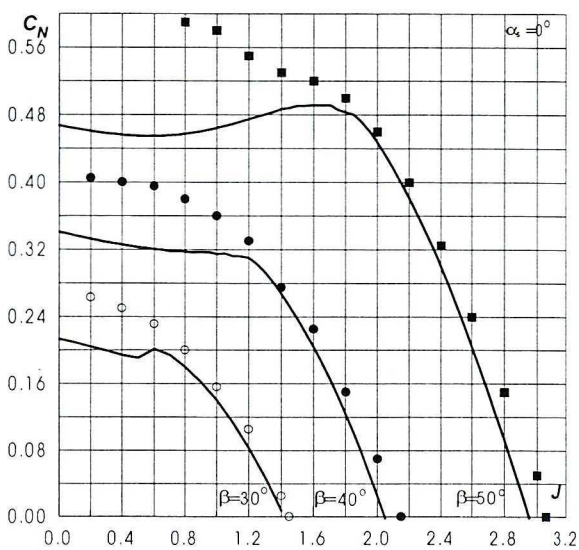

Fig. 5. Power coefficient vs. blade setting angle at *0,75R* and advance ratio for axial inflow conditions

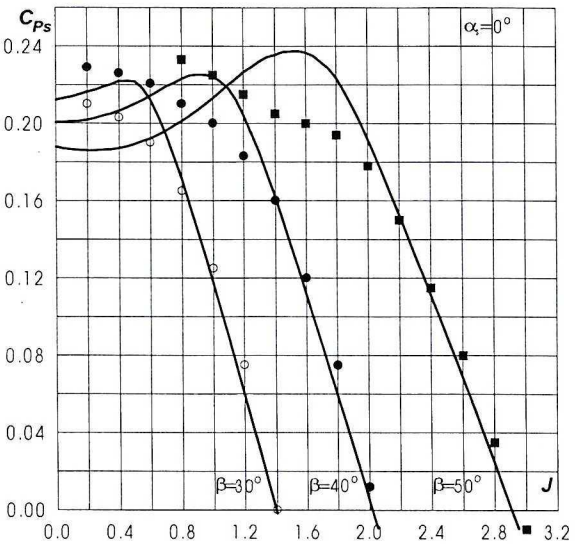

Fig. 6. Thrust coefficient vs. blade setting angle at *0.75R* and advance ratio for axial inflow conditions

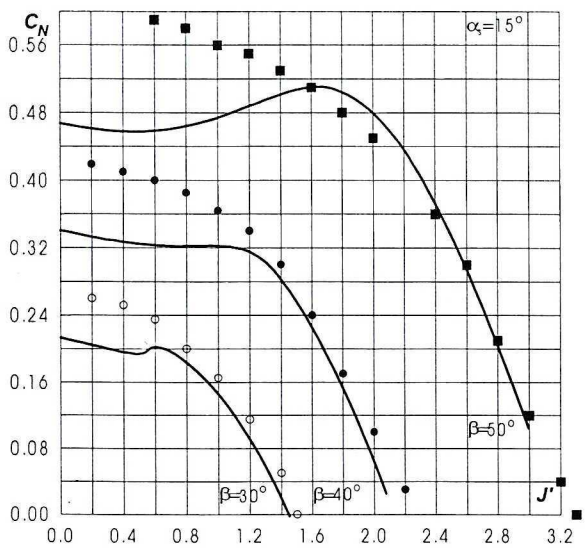

Fig. 7. Power coefficient vs. blade setting angle at *0,75R* and reduced advance ratio *J'*

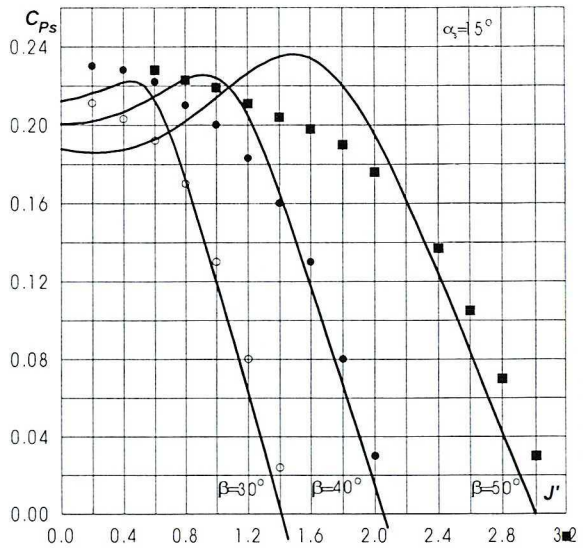

Fig. 8. Thrust coefficient vs. blade setting angle and reduced advance ratio J'

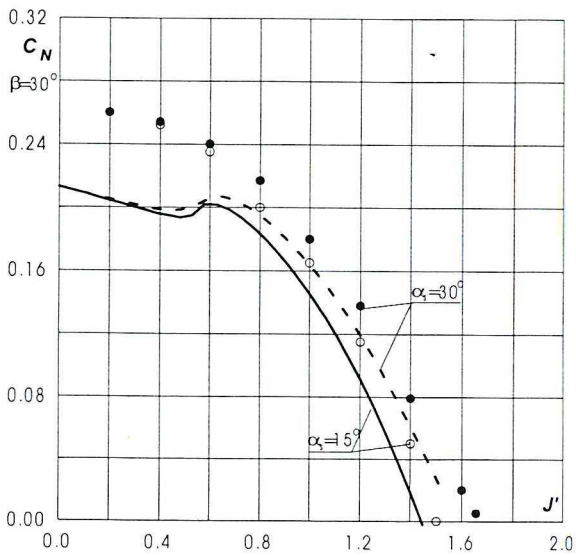

Fig. 9. Power coefficient vs. blade setting angle at *0,75R* and reduced advance ratio J'

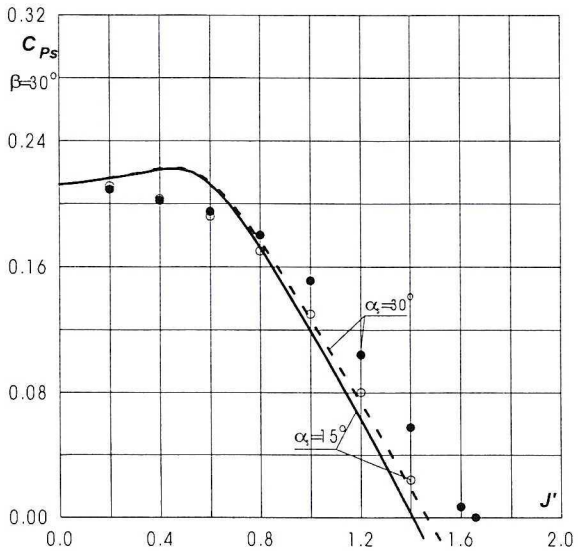

Fig. 10. Thrust force coefficient vs. blade setting angle at *0,75R* and reduced advance ratio *J'*

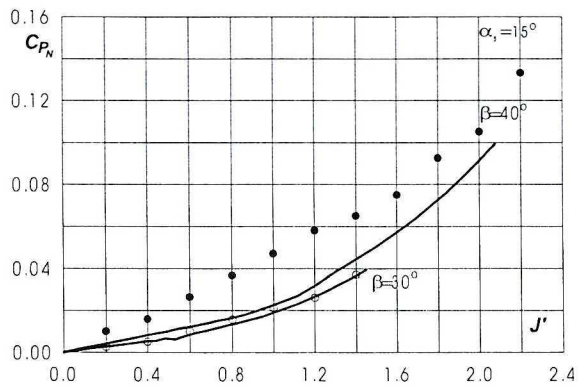

Fig. 11. Normal force coefficient vs. blade setting angle and reduced advance ratio *J'*

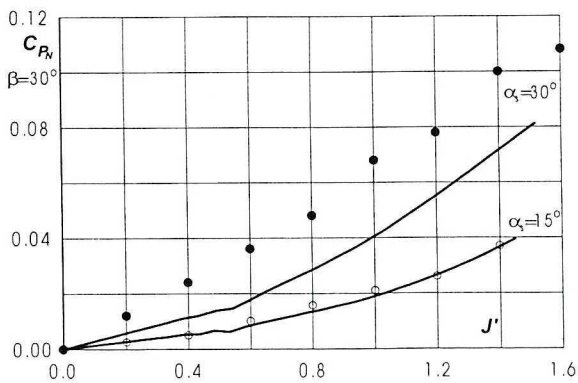

Fig. 12. Normal force coefficient vs. angle of attack and reduced advance ratio *J'*

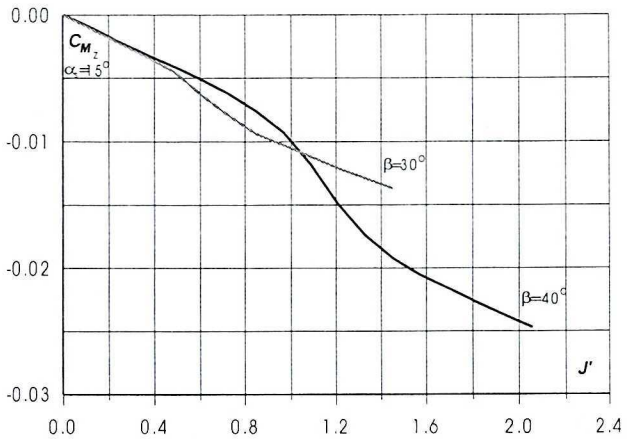

Fig. 13. Propeller yawing moment coefficient for propeller at angle of attack vs. advance ratio J' for the propeller blade settings: $\beta = 30°$ and $\beta = 40°$ at *0,75R*

4. Conclusions an final remarks

The force, moment and power may be calculated accurately for small propeller angles of attack ($\alpha_s < 20°$) employing the presented method. The calculations show very good agreement for thrust and power characteristics as a function of the reduced advance ratio J'. The characteristic of the normal force shows very good agreement with experimental data only for a relatively small blade settings (up to 30°) and angle of attack (see: Fig. 9 and 10). For angles of attack larger than 15°, one may observe the deficiency of the normal force coefficient in comparison with experimental data.

The curve C_{P_N} vs. J' is nearly parabolic. This is similar to the behavior of horizontal force as a function of the advance ratio for helicopter rotor [7]. The normal force coefficient increases as the angle of attack of the blade element decreases, so for large advance ratios the main source of normal force is profile drag of the blade, see eqn. (22). Moreover, for the power curves for axial inflow condition, the power is slightly underestimated. The above suggests that the minimum blade drag was higher then this taken to the present calculations [8]. Because the blade drag has usually small influence on thrust coefficient [3] (see eqn. 21), the thrust curve shows very good agreement with the experimental data. Another source of error may be the too simple model of propeller wake.

Unlike in the case of the small angle approximation presented by Phillips et. al. [13], in this study a dependence of power and thrust characteristics on angle of incidence has been found. However, their results [13] were obtained for angle of attack ± 6° and maximum power coefficient was $C_N \approx 0{,}057$.

[3] Except small advance ratios.

Thanks to the computational simplicity, the present method may be applied to the practical estimation of thrust, power and normal force for propellers.

Manuscript received by Editorial Board, February 27, 2004;
final version, October 04, 2004.

REFERENCES

[1] Baskin W. E., Wil'dGrube L. S., Woshdaev E. S., Maikapar G. I.: Lifting Propeller Theory. Moscow 1973 (in Russian), pp. 126÷128.

[2] Etkin B., Reid L. D.: Dynamics of Flight: Stability and Control,. New York 1996, pp. 336÷440.

[3] Glauert H.: The Elements of Airfoil and Airscrew Theory. Cambridge University Press, Cambridge 1948.

[4] Goldstein S.: On the Vortex Theory of Screw Propellers. Proceedings of the Royal Society A, Vol. 123, 129, pp. 440÷465.

[5] Hall G.: A method of Analysis of Propellers at Extreme Angles of Attack. Journal of Aircraft, Vol. 6, No. 1 Jan-Feb. 1969, pp. 52÷58.

[6] Jarzyna H., Koronowicz T., Szantyr J.: Marine Propeller Design. Selected Problems. Ser. Maszyny przepływowe, T. 20, Ossolineum, Wrocław 1996, pp. 239÷246.

[7] Johnson W.: Helicopter Theory. Princeton University Press, Princeton 1980.

[8] Lindsey W. F.: Aerodynamic Characteristics of 24 NACA 16-series Airfoil at Mach Numbers Between 0.3 and 0.8. NACA TN-1546, September 1948.

[9] McCormick B. W. Jr.: Aerodynamics of V/STOL Flight. Academic Press 1967, pp. 82÷91.

[10] McCormick B. W. Jr.: Aerodynamics, Aeronautics and Flight Mechanics. J. Wiley, New York 1995, pp. 506÷513.

[11] McLemore H. C., Cannon M. D.: Aerodynamic Investigation of Four-Blade Propeller Operating Through Angle-of-Attack Range form 0 to 180 Degrees. NACA TN-3228, June 1954, pp. 1÷62.

[12] Nikolsky A.: Helicopter Analysis. Wiley & Sons, New York 1951, pp. 6÷24.

[13] Phillips W. F., Anderson E. A., Kelly Q. J.: Predicting the Contribution of Running Propellers to Aircraft Stability Derivatives. Journal of Aircraft, Vol. 40, No. 6, Nov.-Dec. 2003, pp. 1107÷1114.

[14] Prosnak W. J.: Determination of the Aerodynamic Characteristics of Propeller. Technika Lotnicza, No. 5/1954, pp. 136÷145 (in Polish).

[15] Ribner H. S.: Formulas for Propellers in Yaw and Charts of Side-Force Derivative. NACA TR-819, 1945.

[16] Roskam J.: Airplane Design Part VI: Preliminary Calculations of Aerodynamic, Thrust and Power Characteristics. DAR Corporation, Lawrence 1990, pp. 337÷343.

[17] Strzelczyk P.: Modification of Witoszyński Theory of Propeller: Influence of Finite Number of Blades. Transactions of The Institute of Aviation, 3/96 (146), pp. 107÷118 (in Polish).

[18] Strzelczyk P.: On Some Form of Lifting Line Equation for Propeller. Transactions of The Institute of Aviation, 2/2000 (161), pp. 87÷92 (in Polish).

[19] Witoszyński Cz.: Selected Papers. PWN, Warszawa 1957, pp. 219÷245 (in Polish).

Wyznaczanie siły normalnej na śmigle w opływie skośnym za pomocą uproszczonej metody wirowej

Streszczenie

W pracy przedstawiono praktyczną metodę wyznaczania charakterystyk aerodynamicznych śmigieł w warunkach napływu skośnego. Zastosowana metoda łączy wyniki uproszczonej metody wirowej z zasadą zachowania pędu i momentu pędu dla przepływu ośrodka idealnego. Dzięki przybliżeniu współczynnika siły nośnej sinusoidą uzyskano zamkniętą postać wzorów na prędkości indukowane. Wyniki obliczeń uzyskane na podstawie przedstawionego w pracy modelu matematycznego zostały porównane z dostępnymi danymi doświadczalnymi. Porównanie to pokazało bardzo dobrą zgodność obliczeniowych charakterystyk ciągu, mocy i siły normalnej z wynikami pomiarów w przypadku kątów natarcia śmigła w przedziale 0–15° i dla szerokiego zakresu kątów nastawienia łopat.

Dzięki swej prostocie opisywania metoda może być z powodzeniem stosowana w praktycznych obliczeniach charakterystyk aerodynamicznych śmigieł.